minerals

MDPI

Article

Pilot Scale Testing of Lignite Adsorption Capability and the Benefits for the Recovery of Rare Earth Elements from Dilute Leach Solutions

Ahmad Nawab and Rick Honaker *

Department of Mining Engineering, University of Kentucky, Lexington, KY 40506, USA; ahmadnawab@uky.edu
* Correspondence: rick.honaker@uky.edu

Abstract: Naturally occurring organic materials containing humic acids show a strong affinity towards rare earth elements (REE) and other critical elements. Leaching experiments on lignite coal waste produced from construction sand production revealed that the contained REEs were associated with the organic matter. Furthermore, adsorption studies revealed that the lignite waste was capable of extracting REEs from a model solution and increased the REE content of the lignite waste by more than 100%. As such, this study aimed to utilize the lignite waste to adsorb REEs from pregnant leach solutions and acid mine drainage sources having low REE concentrations and subsequently leach the lignite material to produce pregnant leach solutions containing relatively high amounts of REEs, which benefits the performance and economic viability of downstream separation and purification processes. An integrated flowsheet was developed based on this concept and tested at a pilot scale. The pregnant leachate solution (PLS) was generated from a heap leach pad containing 2000 tons of Baker seam coarse refuse. The pilot scale circuit was comprised of aluminum precipitation, adsorption using the waste lignite, and rare earth-critical metal (RE-CM) precipitation stages in succession. The results indicated that the aluminum precipitation stage removed over 88% and 99% of the Al and Fe, respectively. The adsorption stage increased the REE content associated with the waste lignite from 457 ppm to 1065 ppm on a whole mass basis. Furthermore, the heavy REE (HREE) content in the feedstock increased by approximately 250%, which raised the percentage of HREE in the REE distribution by 19 absolute percentage points. In addition to the REEs, concentrations of other critical elements such as Mn, Ni, and Zn also improved by 75%, 37%, and 250%, respectively. Bench-scale tests revealed that increasing the solids concentration in the waste lignite and PLS mix from 1% to 20% by weight enhanced the adsorption efficiency from 32.0% to 99.5%, respectively. As such, a new flowsheet was proposed which provides significantly higher REE concentrations in the PLS that can be fed directly to solvent extraction and/or oxalic acid precipitation and, thereby, enhancing process efficiency and economics.

Keywords: rare earth elements; coarse refuse; lignite; humic acid; adsorption; pilot-scale test

Citation: Nawab, A.; Honaker, R. Pilot Scale Testing of Lignite Adsorption Capability and the Benefits for the Recovery of Rare Earth Elements from Dilute Leach Solutions. *Minerals* **2023**, *13*, 921. https://doi.org/10.3390/min13070921

Academic Editor: Sudip Maity

Received: 10 June 2023
Revised: 30 June 2023
Accepted: 6 July 2023
Published: 8 July 2023

1. Introduction

Rare earth elements (REEs) are a group of 17 elements that are classified as light and heavy rare earth elements. Due to their physical and chemical properties, these elements are extensively used in defense, energy, industrial and military technology applications [1]. Globally, REEs are extracted from bastnaesite, monazite, and xenotime. Bastnaesite, which is a rare earth fluoro-carbonate mineral, can be decomposed into rare earth oxides through calcination at high temperatures (>600 °C). However, monazite and xenotime, which are rare earth phosphates, are thermally stable and therefore require chemical treatment at elevated temperatures to ensure complete decomposition [2]. Considering most commercial mineral deposits are in China, significant research is underway globally for rare earth element extraction from secondary sources such as coal and coal by-products.

Various researchers have attempted to physically beneficiate the RE-bearing minerals from coal. However, physical beneficiation processes are inefficient due to the finely disseminated nature of the rare earth particles [3]. Alternatively, hydrometallurgical extraction through acid leaching provides promising means for rare earth element recovery [4]. Researchers have previously conducted investigations on the leaching characteristics of raw bituminous coal from different sources [5–9]. Zhang and Honaker leached the heavier density fractions of Pocahontas No. 3 coal seam at 75 °C using 1.2 mol/L HCl and 1% S/L ratio for 5 h. It was determined that the total rare earth element (TREE) recovery was only 14% even after leaching with high strength acids [10]. Zhang and Honaker also conducted another investigation on the leaching characteristics of the heavier density fractions of Baker, Fire Clay, and Illinois No. 6 coarse refuse seam material using previously mentioned leaching conditions and reached the same conclusion that direct leaching of the untreated bituminous coal did not provide appreciable TREE recovery [11].

Alternatively, it was determined that the calcination of Fire Clay and Baker seam materials at elevated (~600 °C) temperatures improved REE recovery. The benefits were realized by liberating rare earth-bearing minerals through decarbonization, clay dehydroxylation and/or decomposition of rare earth-bearing minerals in a soluble form [11]. However, even though the calcination pretreatment improved light REE (LREE) recovery, heavy rare earth element (HREE) recovery did not change significantly [12,13]. It was found that most of the LREEs in the Fire Clay seam coal existed as monazite whereas HREEs were associated with xenotime and zircon, which are thermally stable minerals [14]. As such, thermal treatment in the presence of chemicals was crucial to realize high TREE recovery [15].

Compared to bituminous coal, which requires stringent treatment conditions for high REE recovery, mild acid leaching can recover REEs in lignite coal. This is due to the REE association with the organic matter, such as humic acids in the lignite coal instead of mineral matter. As per Szymanski et al., humic acids are compounds characterized by a high level of phenol hydroxyl and carboxyl groups which cannot be represented by any single formula due to their complexity [16,17]. Laudal et al. reported >80% REE recovery from Fort Union lignite coal using 0.5 mol/L sulfuric acid [18]. REEs in lignite coal are primarily associated with organic matter such as humic acids (HAs). Due to their strong affinity towards rare earth elements, HAs have been extensively studied in recent years and several models have been developed to simulate their adsorption behavior [19]. Researchers have conducted several investigations on the bench scale for rare earth adsorption using humic acids [20–22]. Similarly, the adsorption capabilities of humic acids have been exploited in other industries [23,24].

This investigation assessed the potential to enhance REE concentration selectively in pregnant leach solutions (PLS) generated from secondary sources such as coal waste and acid mine drainage solutions using lignite waste generated from construction sand production. The particular lignite waste material used in the study had a TREE content exceeding 400 ppm as well as elevated amounts of cobalt, nickel, and zinc. The primary PLS in the study was provided by an active heap leach comprised of bituminous coarse coal waste material. Since no prior treatment of the lignite waste is necessary and REE extraction from the lignite waste is possible through mild acid, the downstream process efficiency gains from treating PLS containing greater amounts of REEs, and other critical elements are anticipated to provide relatively favorable economics. Based on the outcome of the study, a potential flowsheet is presented, which can be employed to extract and purify rare earth elements.

2. Materials and Methods

2.1. Materials

The lignite was tailings material from a construction sand operation in Missouri, USA. Approximately 20 tons of lignite material was provided for the test program. The total rare earth element (TREE) content measured using inductively coupled plasma optical emission spectroscopy (ICP-OES) revealed that the material contained 380 ppm on a whole

mass basis. However, the majority of the material finer than 0.6 mm was sand with only 73 ppm TREE content and 98% ash content. As such, the material was screened at 30 mesh. The TREE content was upgraded in the screen overflow to 457 ppm (Tables 1 and S1). Additionally, the material contained elevated Ni, Co, Mn, and Zn contents compared to other bituminous coal sources discussed in this investigation. Elevated concentrations suggest that the lignite material is an attractive source of these critical metals. The overflow material was crushed to a top size of 1 mm using a hammer mill and used as feed for the tests.

Table 1. Elemental content in the lignite material screened at 30 mesh measured using ICP-OES.

TREE	Co	Ni	Zn	Mn
456.5	281.7	919.8	185.8	420.2

The pregnant leachate solution (PLS) used in this study was generated from leaching 2000 tons of coarse refuse generated from the processing of Baker seam coarse refuse, which is a bituminous coal source. A sample of the refuse was characterized utilizing XRD, XRF, and ICP-OES. The XRD data indicated that quartz, kaolinite, illite/muscovite, and pyrite were the primary mineral phases in the refuse material (Figure 1). Similarly, the XRF analysis revealed elevated silica and aluminum oxide concentrations due to the clays such as kaolinite and illite (Table 2). It was also found that there was 18.97% Fe_2O_3 content because of the high pyrite concentrations in the material. Elemental analysis using the ICP-OES revealed that the material contained 387 ppm of TREEs, of which 13.7% were heavy REEs (Yttrium, Dysprosium, Terbium, Holmium, Erbium, Thulium, Ytterbium, Lutetium) (Table 3). Compared to the lignite material, the Baker seam coarse refuse contained Co, Ni, Mn, and Zn content of only 25 ppm, 56 ppm, 218 ppm, and 130 ppm, respectively.

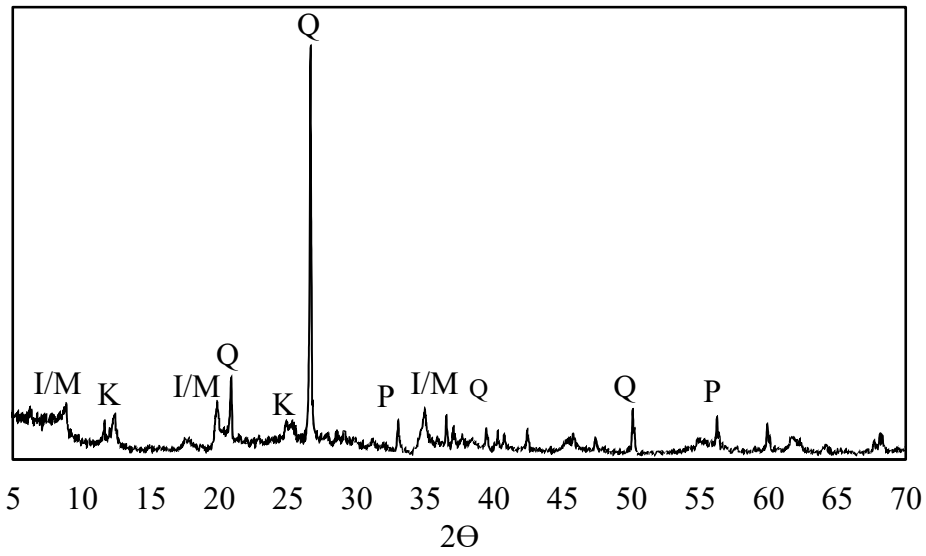

Figure 1. XRD analysis of the Baker seam coarse refuse material (Q: Quartz, K: Kaolinite, I/M: Illite/Muscovite, P: Pyrite).

Table 2. X-ray fluorescence (XRF) analysis of major and minor mineral phases in the Baker seam coarse refuse material.

	SiO_2	Al_2O_3	Fe_2O_3	CaO	MgO	MnO	K_2O	P_2O_5	TiO_2	BaO	SrO	SO_3
Coarse Refuse	50.49	22.76	18.97	0.74	1.19	0.05	3.52	0.17	0.95	0.05	0.07	1.04

Table 3. REE concentration (whole mass basis, ppm) in the Baker seam coarse refuse material.

Sc	Y	La	Ce	Pr	Nd	Sm	Eu	Gd
21.94	34.71	62.28	138.29	15.85	61.58	20.82	2.2	10.35
Tb	**Dy**	**Ho**	**Er**	**Tm**	**Yb**	**Lu**	**LREE**	**HREE**
2.4	6.95	0.73	2.87	0	4.72	1.25	333.31	53.63

Construction of the heap started with the installation of geosynthetic clay liners, perforated drains, and overliners (Figure 2A) followed by the loading of the coarse refuse material (Figure 2B) on the heap pad. Locally sourced river rock, a silica-based material, was selected for the overliner to allow proper flow to the PLS collection basin without being a source of contamination due to leaching. Locally generated acid mine drainage (AMD) and the addition of sulfuric acid to achieve a solution pH of 1 were used to initiate leaching in the heap. Afterward, acid production from the bio-oxidation activity naturally generated the desired leaching action and prevented precipitation issues. Heap irrigation was achieved using a drip tube system to achieve a 0.20 lpm/m^2 (0.005 gpm/ft^2) irrigation rate, which equated to a PLS flow rate of 80 lpm (21 gpm). The heap leach PLS was collected in a basin (Figure 2C), and the solution pH, Eh, and REE content were measured daily using an on-site ICP-OES. To ensure proper mixing of the PLS, extra irrigation driplines were fitted to a compressed air manifold and placed into the heap sump. For each test, the PLS was transferred into storage tanks (Figure 2D) and subsequently moved inside the processing facility for continuous pilot scale testing [25].

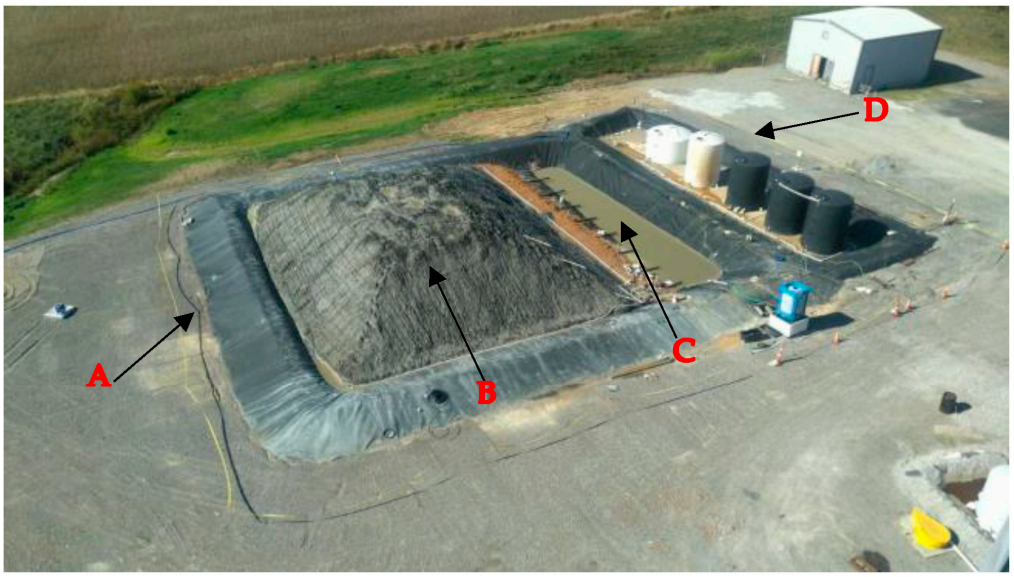

Figure 2. Aerial view of the baker seam coarse refuse heap (A) HDPE plastic liner, (B) Coarse refuse material, (C) Collection Pond, (D) Storage tanks.

Industrial-grade sulfuric acid and sodium hydroxide purchased from Chemstream were used in the laboratory and pilot plant tests. Sulfuric acid was 93 wt.% whereas NaOH was 50 wt.% content. Trace metal-grade sulfuric acid purchased from Fischer Scientific was used for bench-scale experiments. The desired chemical concentration solutions were prepared with de-ionized (DI) water with a resistivity of 18 MΩ-cm. Bench scale experiments were conducted using a magnetic stirrer purchased from Cole-Parmer.

2.2. Methods

2.2.1. Leaching

The laboratory leaching studies were carried out in a three-neck round bottom flask, which was submerged in a heated water bath to maintain the desired solution temperature. Heated plates coupled with external water heaters purchased from Cole-Parmer (SHP-200, Vernon Hills, IL, USA) were used to increase the solution temperature, which was measured continuously using a thermometer to ensure a consistent temperature. Additionally, since elevated temperatures can cause a loss in volume, the flask was connected to a reflux condenser to minimize volume loss during the experiments. All experiments were performed using the same stirring speed and magnetic stir bars. The slurry samples collected from each experiment were dewatered using a 0.45-µm PVDF membrane filter. The solution pH was monitored using an Orion™ Versa Star Pro™ pH meter from Thermo Scientific (VSTAR12, Waltham, MA, USA), which was calibrated using pH 1.68, 4.01, and 7.00 buffer solutions purchased from Cole Parmer (Vernon Hills, IL, USA). A P4 medium-fine porosity filter purchased from Fisher Scientific (version, Hampton, NH, USA) with a slow flow rate was used to filter the residual slurry. The filtered cakes were air-dried in an Heratherm oven (OMS180, Thermo Fisher Scientific, Waltham, MA, USA) oven at 70 °C for 12 h. The dried samples were weighed, and the values recorded. Bench scale adsorption tests were conducted in the same manner as leaching experiments but at room temperature.

2.2.2. ICP-OES Analysis

Elemental analysis on the liquid and solid samples was conducted using inductively coupled plasma optical emission spectroscopy (ICP-OES, Spectro, Kleve, Germany). The liquid samples were diluted to 10× and 100× using 5% HNO_3 to reduce the elemental content to within the detection limit of the instrument. The solid samples were ashed using a LECO 701 thermogravimetric analyzer (Benton Harbor, MI, USA), and the subsequent samples were digested using a modified ASTM D6357-11 method. The resulting liquid was diluted to 20× for the same reason as described previously.

The instrument was calibrated using a multi-element reference standard, VHG SM68 standard 1, at 0-, 0.05-, 0.5-, 1-, 5.0-, and 10-ppm concentrations in a 5% HNO_3/H_2O matrix. In between any two samples/calibration standards, a 10% HNO_3 solution was used for rinsing to avoid any cross-contamination of the samples. Following the calibration, Spectro software was employed to set the peak position to account for any signal drift, and a linear regression model was applied to the calibration points. The minimum correlation coefficient was set at >0.996 for each element and if the criteria did not meet, the instrument was recalibrated. Synthetic solutions of known concentrations were used to ensure high instrument accuracy (±10% relative standard deviation). Finally, the calibration accuracy was consistently checked after 17 samples to limit any deviation in the results.

The leaching recovery values were calculated using the following formula:

$$\text{Leaching Recovery } (\%) = \frac{C_L \times V_L}{C_L \times V_L + C_{SR} \times M_{sr}}$$

where C_L and C_{SR} are the concentrations (ppm) in the leachate and solid residues, respectively, V_L the PLS volume (L) and M_{SR} the solids mass (kg).

2.2.3. X-ray Diffraction

Mineral phases in the Baker seam coarse refuse material were identified using a Bruker instrument (Advance D8, Bruker, Billerica, MA, USA). For each XRD analysis, a powdered sample was compressed into a disc pellet and analyzed at 1 degree/min from 10 to 70 degrees. Subsequently, DIFFRAC EVA software (version number) was employed to identify the mineral phases in the XRD spectra.

3. Results and Discussion

3.1. Bench-Scale Experimentation

3.1.1. Leaching Study

To identify the leaching characteristics of the lignite waste material, a series of leaching experiments were performed over a range of sulfuric acid concentrations at 1% S/L (*w*/*v*), 75 °C for 2 h. All the leaching parameters were employed to provide a direct comparison between the extensive leaching studies reported previously from different coal sources [15,26,27]. It was determined that mild acid-leaching conditions could be used for REE extraction without any thermal treatment (Figure 3). Rare earth element recovery improved from 32% to 88% when sulfuric acid concentration increased from 0.01 mol/L to 0.1 mol/L. A further increase in sulfuric acid concentration to 0.5 mol/L increased the REE recovery to 96%. Additionally, a leaching experiment using 1.0 mol/L ammonium sulfate as the lixiviant recovered only 5% REEs, implying that most REEs arion-exchangeable exchangeable form [28]. The individual REE recoveries at various sulfuric acid concentrations are presented in Figure S1.

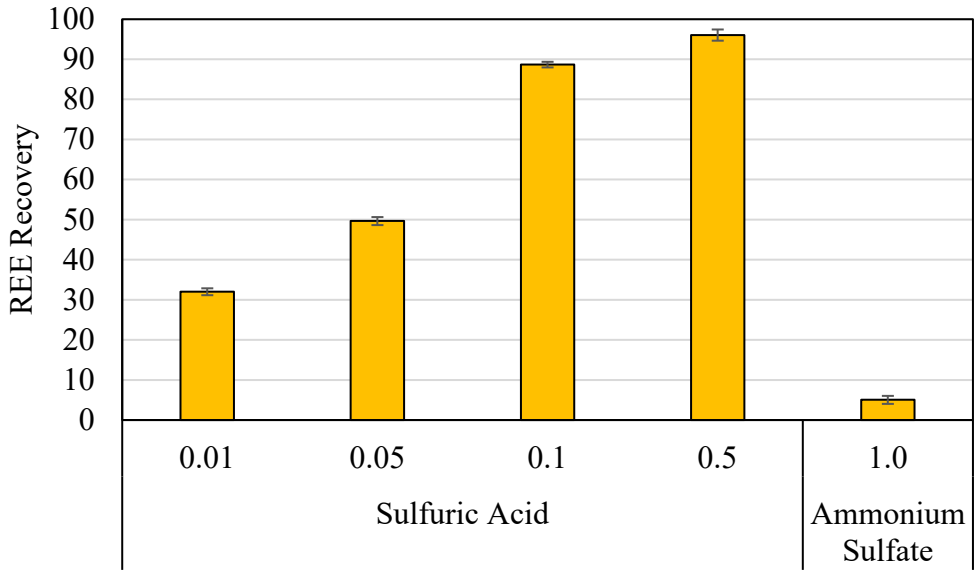

Figure 3. Leaching characteristics of rare earth elements as a function of lixiviant type and strength (mol/L).

For bituminous coal sources, it has been well reported in the literature that REEs associated with mineral matter such as clays generally require relatively strong acid conditions [3]. Thermal treatment is typically required to liberate the REE-bearing minerals through decarbonization, clay dehydroxylation and decomposition of liberated REE-containing minerals into a soluble form [10]. For instance, Zhang et al. reported that TREE recovery of Baker seam coal refuse increased from 24% to 79% following thermal treatment at 600 °C for 2 h using 1.2 mol/L HCl [11].

The recovery from the lignite source resulted in 85% of the REEs reporting to the pregnant leach solution using 0.1 mol/L sulfuric acid. The leaching results suggested that the REEs in the lignite were likely not associated with the mineral matter. Previous research has shown that the REEs associated with organic matter as opposed to mineral matter are susceptible to a mild acid attack [18]. Rare earth elements, especially HREEs, have a strong association towards the organic matter in coal [29]. Since lignite coals are rich in humic acids which chelate more strongly with HREEs as opposed to LREEs, it was hypothesized by Laudal et al. that HREEs in lignite were primarily associated with the organic matter [30]. In contrast, LREEs were likely associated with both organic matter as well as acid-soluble mineral forms such as sulfates, carbonates, and oxides [18].

3.1.2. Adsorption Study

Since rare earth elements show a strong affinity towards organic matter such as humic acids, it was hypothesized that the waste lignite that was naturally enriched in REEs could potentially be used for REE adsorption from a dilute solution to further elevate its REE content [31–33]. As such, to confirm this hypothesis, a stock solution of known concentration was mixed with solids at a 20% S/L (w/v) ratio for 20 min. The synthetic solution was prepared with 5% hydrochloric acid and the solution pH was increased to 2.0 using sodium hydroxide (Table 4). These operating parameters were selected simply as a starting point for the study.

Table 4. The concentration of different elements in the stock solution prepared from metal chloride standards.

	TREE	Sc	Y	Nd	Gd	Al
Stock Concentration (ppm)	75.19	17.4	19.31	18.46	20.02	1499

The initial test was performed by mixing the untreated material with the stock solution. It was found that the untreated solids had significantly high adsorption efficiency for all elements added to the model system (Figure 4). For instance, scandium removal from the solution was 65%, whereas Nd and Gd adsorption efficiency was 55% and 52%, respectively. These results confirmed the hypothesis that the REEs from the solution could be adsorbed on the lignite. Interestingly, the adsorption efficiency for aluminum was approximately 25.9%. Since the initial concentration of Al was 20× higher than the REEs, the absolute concentration adsorbed for Al would be much higher than the REEs. Therefore, it is likely the aluminum ions preferentially consumed the rare earth binding sites, which contributed to a lower adsorption efficiency for REEs [34,35]. A more detailed discussion on this subject is presented later in the paper. Interestingly, due to elevated calcium content in the solids, which increased the neutralization potential of the solids, the solution pH drifted from 2.0 to 3.9 within the first five minutes of the reaction. Since the aluminum precipitation from the PLS starts at 3.5 and accelerates exponentially to 4.5, a portion of the adsorption efficiency increase for aluminum may be contributed by its precipitation at the higher pH levels [36]. However, since REE precipitation is minimal at pH 4.0 in a sulfate system, the reported adsorption efficiency for REEs is not expected to be influenced by their precipitation.

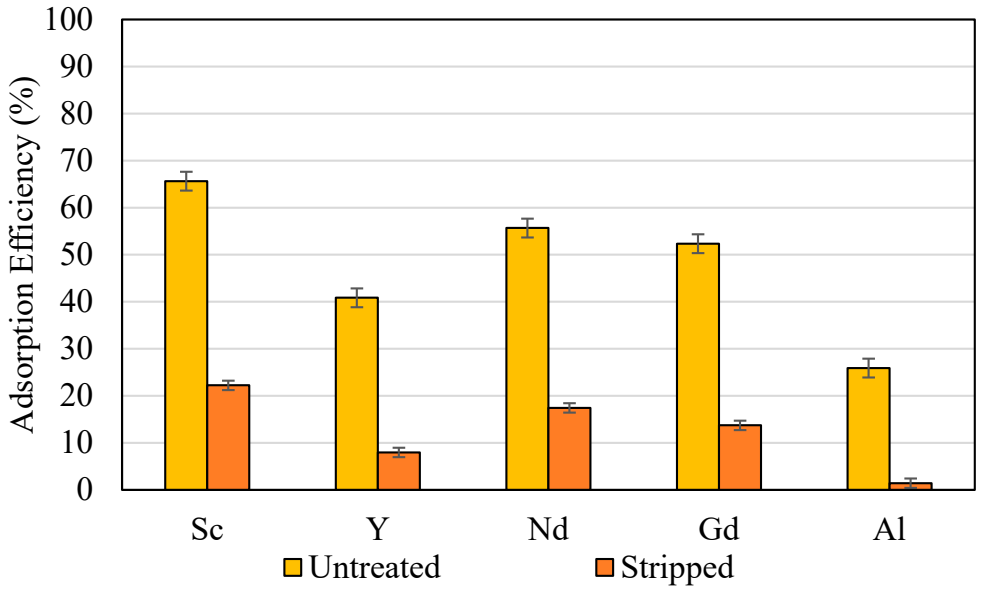

Figure 4. Adsorption efficiency of different elements from the stock solution onto the untreated and stripped solids (Stripped: Treated with 0.5 mol/L sulfuric acid).

As the solution pH can influence the adsorption efficiency of rare earth elements, another test was conducted where the material was leached with 0.5 mol/L H_2SO_4 to remove calcium using the same conditions presented previously. The solid residue was thoroughly washed with de-ionized water, air-dried, and subsequently used for the second experiment, which was conducted in the same manner as the first one. Due to the addition of a calcium stripping stage, the pH of the solution drifted only from 2.0 to 2.43 at the end of the reaction. Interestingly, it was found that the adsorption efficiencies for REEs and Al also dropped significantly. For instance, scandium adsorption efficiency dropped from 65% to only 22%. Various researchers have demonstrated a significant decrease in adsorption efficiency as a function of solution pH with the lowest efficiencies below 2.5 pH [19,37,38]. Marsac et al. reported competitive binding of H^+, Al^{3+}, and Fe^{3+} ions in the acidic pH range [19]. Considering a logarithmic increase in H^+ concentrations with a decrease in pH, relatively low adsorption efficiency in the second test was likely due to the preferential binding of hydrogen ions to the adsorption sites.

3.2. Continuous Pilot-Scale Study

3.2.1. Process Design

Preliminary lab-scale experiments revealed favorable REE adsorption characteristics of the lignite material employed in this investigation. The findings from the bench scale experiment inspired the design of a pilot scale test with an aim to generate a concentrated REE feedstock for hydrometallurgical extraction. This proposed process can use acid mine drainage (AMD) or any other solution as a REE source. Since both AMD and the lignite material used in this investigation are typical waste products from two separate and distinctly different operations, the proposed process provides a means to benefit from the treatment of AMD, which is an environmental hazard, while generating a potential feedstock for the recovery of rare earth elements and other critical elements using hydrometallurgical methods.

As previously described, the primary REE source for this investigation was a PLS generated from a heap leach test pad containing a bituminous coal coarse refuse. The concentrations of different elements in the PLS are shown in Table 5. The results indicated that the PLS contained elevated concentrations of contaminants such as Al, Ca, and Fe compared to REEs (Table 5). It has been reported in the literature that these contaminants compete with REEs for binding sites [19]. Therefore, adding a contaminant removal step prior to the adsorption stage was crucial to maximize the REE adsorption characteristics of the lignite waste material. As such, a precipitation study was conducted on the heap leach PLS to identify the optimal set points for contaminant removal (Figure 5). The results demonstrated that most of the Al and Fe precipitated at pH 4.5, and increasing the pH above this setpoint resulted in considerable REE losses. Therefore, following the Al and Fe removal, adsorption was also completed at the same pH value. The objective of the adsorption stage was to provide a concentrated REE feedstock for downstream separation and purification processes. Since REEs can potentially be concentrated in a smaller mass of solids which will reduce the total volume needed to be treated by the downstream processes, significant reductions in capital and operating expenses (CAPEX and OPEX) may be realized.

Table 5. Concentrations (ppm) of various elements of interest in the heap leach PLS used as a feedstock for the study.

TREE	Co	Ni	Zn	Mn	Al	Ca	Fe
19.8	10.1	33.4	42.0	134.2	2343.2	477.9	3377.6

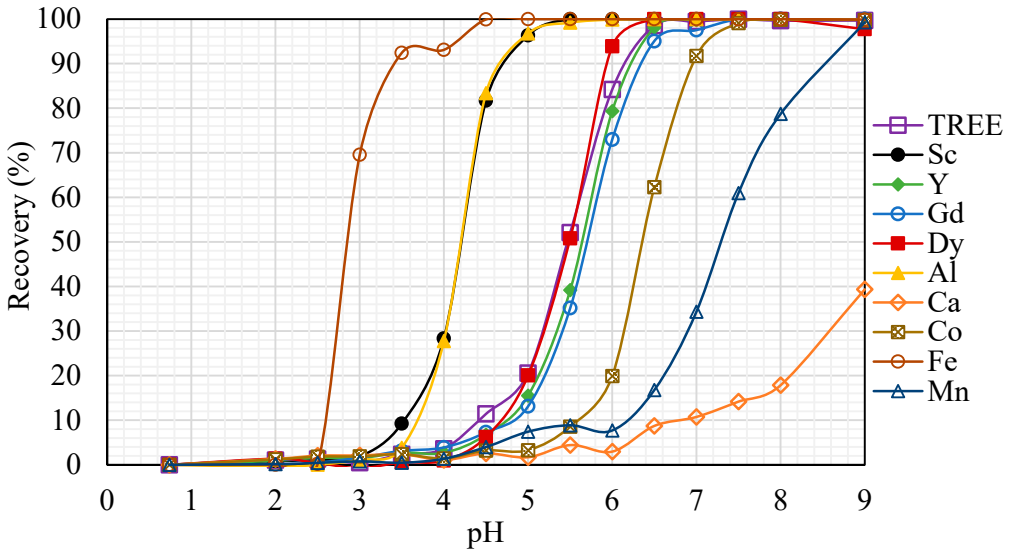

Figure 5. Precipitation behavior of elements of interest from heap leach PLS using NaOH as pH modifier.

3.2.2. Pilot-Scale Test

For this experiment, heap leach PLS was fed to a 340-L mixing tank at 7.6 lpm using a pneumatic diaphragm pump (Figure 6). The tank contained Eh (a measure of the redox potential) and pH probes, which were connected to an online feedback PLC controller capable of altering the peristaltic pump speed. The PLC system maintained a pre-determined pH setpoint by manipulating the pump speed used to inject a 4 mol/L NaOH stock solution into the mixing tank. The reactor tank overflow was mixed with a 0.1% flocculant solution using an inline mixer and subsequently discharged into a 1500-L thickener. Underflow from the thickener was dewatered using a high-pressure plate filter press operated at 684 kPa.

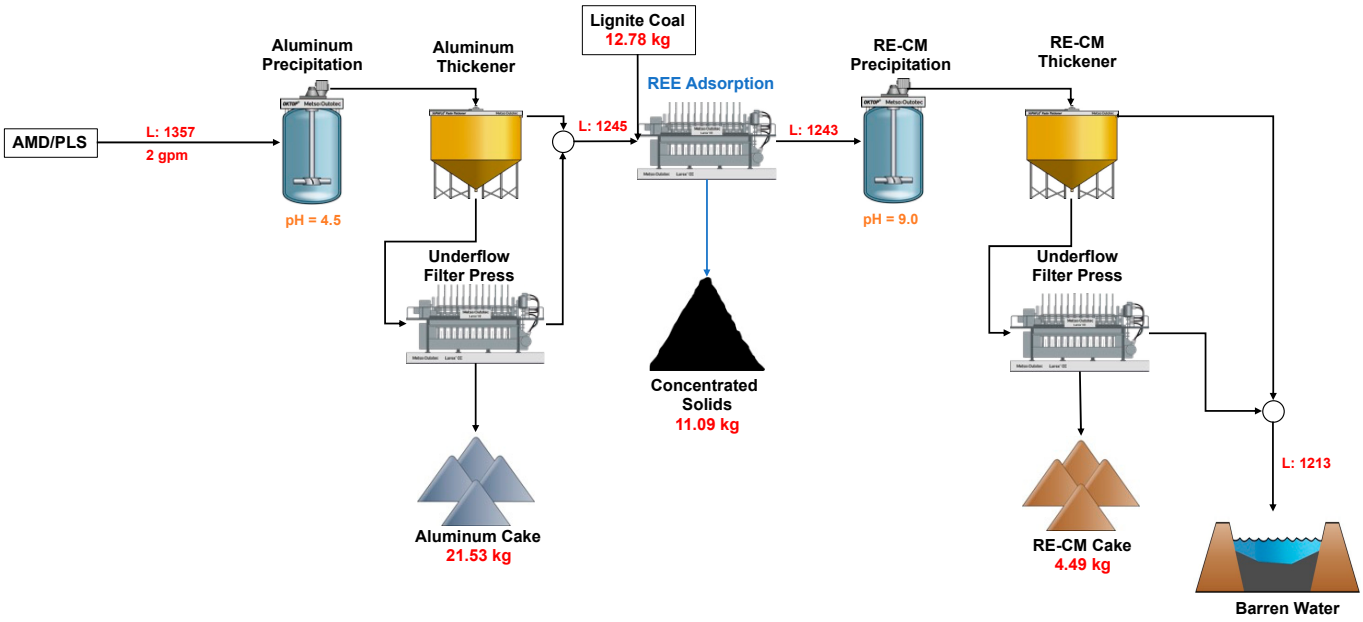

Figure 6. Circuit schematic for the pilot-scale test for rare earth adsorption and contaminant removal (masses on a dry basis, L: liquid, Flowsheet built using HSC Chemistry 10).

During the solid-liquid separation of aluminum precipitate, raffinate from the filter was monitored continuously. The filter operation was stopped upon observation of particles in the filtrate and the solids removed. The overflow from the thickener was combined

with the filtrate and used for feed to the next stage. For the REE adsorption tests, the filter plates were packed with the lignite material by pumping a 20% S/L slurry through them in a closed loop until the discharge water was clear. Subsequently, the REE-containing solution was passed through the packed bed, and the filtrate was pumped to the RE-CM precipitation stage. The pH of the filtrate was adjusted by the online control system to a value of 9, which caused precipitation of any remaining REEs and other critical elements such as cobalt, nickel, and zinc. The precipitates were recovered using an identical thickener-plate filter press arrangement as described for the aluminum precipitation circuit. The filtrate from the RE-CM operation was discarded as wastewater.

3.2.3. Data Reconciliation

The final volumes from the pilot-scale test were estimated based on the pump flow rates, whereas masses were estimated by weighing the filter cakes. Any base added during the test was automatically recorded in the OSIsoft PI system, which was later used in the calculation. Liquid samples were collected from the feed and the raffinate of each unit operation along with solid samples from the filtered cakes. As the solid samples contained significant moisture content, they were air-dried in the oven for 12 h, and the dried samples were collected for digestion. Samples were weighed before and after drying to determine the solid content of the cake. The samples were analyzed using ICP-OES, and the weighted sum of squares (WSSQ) was employed to obtain a complete mass balance around the circuit using the following formula:

$$\mathrm{WSSQ} = \sum_{k=1}^{c}\sum_{i=1}^{m}\left(\frac{a_i^{k^*} - a_i^k}{S_i^k}\right)^2 + \sum_{i=1}^{m}\left(\frac{M_i^* - M_i}{S_i}\right)^2$$

$$S_i^k = e_i^k a_i^k$$

$$S_i = e_i a_i$$

where a_i^k and M_i are the actual assay and mass flow rate values, S_i and S_i^k the standard deviation in mass flow and assay for stream i and component k, e_i and e_i^k the relative error in mass flow and assay for stream i and component k, and * indicates estimated values.

3.2.4. Test Results

The results indicated that the aluminum precipitation circuit operated with a pH setpoint of 4.5 effectively removed most of the iron and aluminum from the solution (Figure 7) as indicated by Fe and Al recovery values of 88% and 98%, respectively. However, it should be noted here that there was a 30% loss of rare earth elements in the aluminum precipitation stage. This was likely due to the adsorption of rare earth elements on the surface of Fe-precipitates to neutralize its surface charge [36]. Typically, Al^{3+} ions in the solution can neutralize the charge. However, if the concentration of Fe is significantly higher than Al, which is the case for the given PLS (Table 5), a loss of REEs occurs. To minimize this effect, separate Fe and Al precipitation stages are required. Since ferric iron precipitation at pH < 3.5 is below 85%, there should be enough Al in the system to neutralize its surface charge for the given PLS, hence, minimizing the REE loss.

The adsorption efficiency for REEs, Mn, Ni, and Zn in the test was approximately 32%, 17%, 10%, and 9%, respectively (Figure 7). The contaminants ions, such as Al and Fe, showed relatively higher precipitation efficiencies compared to REEs. Since it is not possible to distinguish between elements adsorbed and precipitated at this stage, it is anticipated that at least some of the Al and Fe adsorption efficiency increase was caused by simple precipitation of these elements in this pH range. Interestingly, there was no adsorption of Ca and Co. In fact, both elements were leached from the solids with 43% and 2% recoveries, respectively. Removal of significant calcium concentration in this stage is anticipated to provide economic benefits with respect to chemical consumption when

treating this feedstock for hydrometallurgical extraction. Finally, increasing the solution pH to 9.0 removed the remaining elements of interest from the solution. Since most of the calcium precipitates in the basic pH range above 9 (Figure 4), its precipitation efficiency was lower than other elements. However, it should be noted that considering the prior leaching of Ca in the adsorption stage, a small percentage of calcium in the cake will translate into significant content due to its elevated concentration in the feed solution.

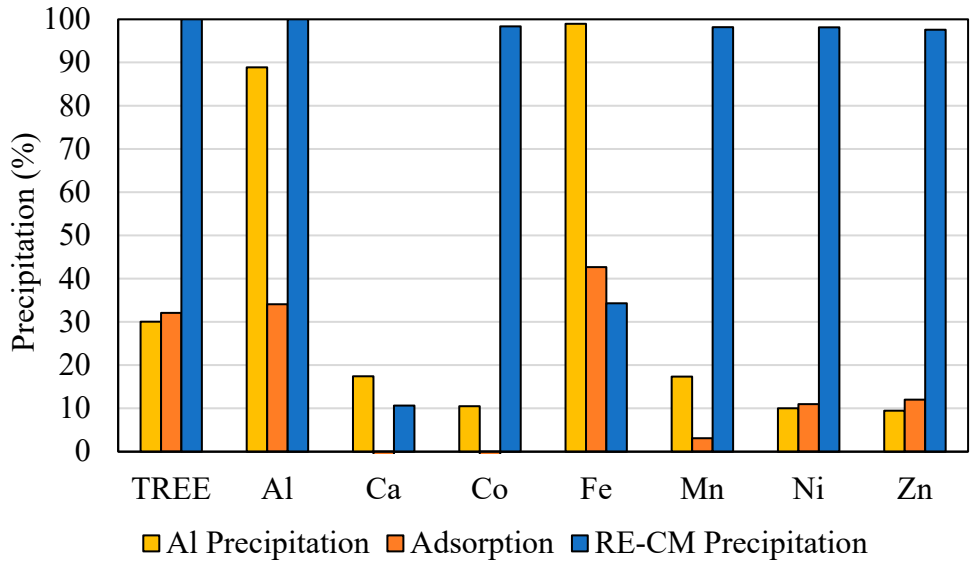

Figure 7. Recovery of various elements in the aluminum precipitation circuit, the lignite adsorption process and the RE-CM precipitation circuit of the pilot plant.

Considering distinct mass losses in the different precipitation stages along with the elemental assays of the cakes, unit recovery values do not provide complete information. Therefore, it is crucial to normalize the complete data set relative to the feed content i.e., mass distribution/overall recovery values. For instance, it is evident from the data shown in Figure 8 that almost all the Fe and most of the Al were precipitated in the aluminum precipitation stage. Similarly, rare earth elements removed from the PLS in the adsorption stage represented approximately 22% of the TREEs present in the system. Most of the REEs and other critical metals are reported to the RE-CM cake, which is a result of low removal efficiencies in the adsorption stage. It is likely that low REE removal during the adsorption stage was due to the significantly lower solid content relative to the volume of the PLS and/or, the limited residence time provided in the filter for adsorption. A more detailed discussion is provided later in this publication.

It is worth mentioning here that a RE-CM precipitation step is typically required when treating dilute PLS to generate a concentrated feedstock for downstream processing. The anticipated outcome from this precipitation stage is to provide a concentrated RE solution from the leaching of RE-CM cake, which can be processed using either solvent extraction and/or oxalic acid precipitation to generate high-purity products. However, it was found that, even though most of the REEs and CM were precipitated at pH 9.0, the filtered precipitates retained approximately 80% water content. As such, when leaching the RE-CM cake, the excessive water content caused the REE content in the solution to drop significantly. Unfortunately, it was observed during plant operation from other pilot tests that reducing the external water content during leaching was not an option as the REE-leaching efficiency was significantly impacted. Comparatively, the lignite material following adsorption retained only 22% water content. Therefore, high solids leaching of the material was anticipated to provide a significantly higher REE and CM content in the PLS, which is ideal for solvent extraction and/or oxalic acid precipitation.

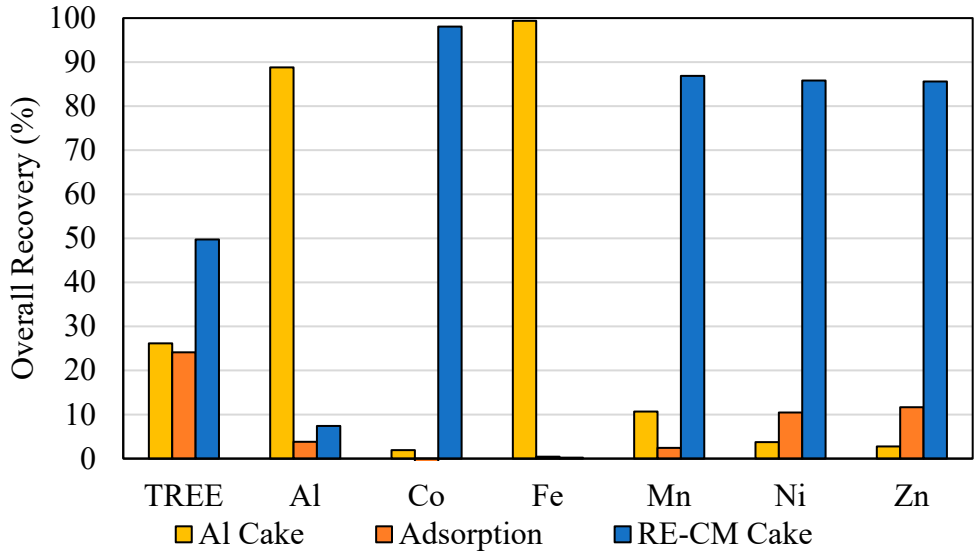

Figure 8. Overall recoveries achieved in the aluminum precipitation circuit, the lignite adsorption process, and the RE-CM precipitation circuit of the pilot plant.

3.2.5. Improvement in Feedstock

After the adsorption test, the lignite was analyzed for elemental content. Comparing the elemental concentration after adsorption to the initial values revealed that the TREE content increased by more than 100%, with HREE content improving by 250 percent (Figure 9). The overall REE content increased from 457 ppm to 1065 ppm on a whole mass basis. Considering the criticality of heavy REEs such as dysprosium, yttrium, and terbium in the development of clean energy technologies, the results suggest that the proposed flowsheet can provide promising means to improve the concentrations of these elements. This statement is supported by the REE content data shown in Table 6, which clearly demonstrates a significant change in the rare earth distribution. Initially, LREE represented approximately 74% of REE content in the feed which changed to 55% after adsorption. Similarly, Mn, Ni, and Zn concentrations also improved with Zn content increasing by more than 250 percentage points. Additionally, as the Co leaching recovery was approximately 2%, no significant cobalt content was lost during this process.

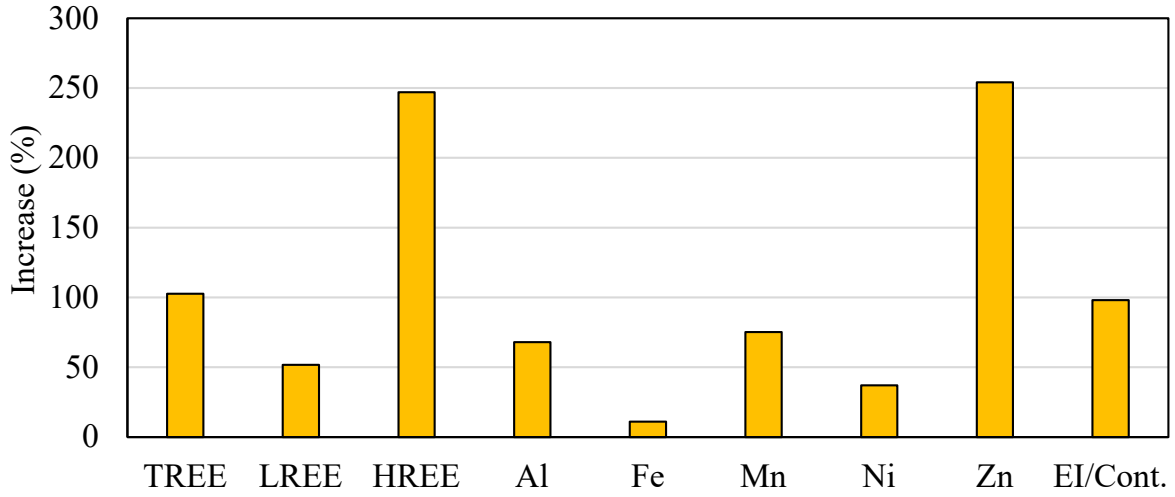

Figure 9. Percent improvement in the concentrations of different elements and EI/Cont. in the concentrated solids relative to feed solids. (EI/Cont. = Elements of interest/Contaminants).

Table 6. Comparison of the elemental content in the feed solids and the concentrated solids (whole mass basis, ppm).

	TREE	LREE	HREE	Al	Ca	Co	Fe	Mn	Ni	Zn
Feed Solid	457	338	118	13,809	24,292	282	14,409	420	920	186
Concentrated Solids	1065	590	465	26,714	6639	299	18,426	848	1451	758

Furthermore, the data demonstrated a 67% and 11% increase in the Al and Fe content, respectively. Interestingly, even though overall concentrations of these contaminants increased, there was approximately a 100% improvement in the ratio of elements of interest and the total contaminants in the feed. An increase in this ratio indicated that the feedstock was upgraded with fewer contaminants relative to the elements of interest. This change was due to the major reduction in the calcium content, which was present as calcite and was effectively removed by contact with a very mild acid (Table 6). Since the calcite is readily soluble and acts as a neutralizing agent, its removal is anticipated to provide improvement in the chemical cost as well as the final purity of the rare earth oxide product, which can be negatively impacted by the precipitation of calcium oxalate [39].

3.2.6. REE Improvement Pattern

REEs have been shown to bind to carboxylic, phenolic, and chelating ligands. To be more specific, LREEs preferentially bind to carboxylic acids such as acetic acids whereas HREEs bind to phenolic and other chelating ligands [35]. However, other ions such as Al^{3+}, Fe^{3+}, and H^{+} compete with REEs for the binding sites. The competitive effect of contaminant ions changes as a function of pH and REE/HA ratios resulting in distinct distributions of REEs in different deposits/solutions [19,37]. For instance, Marsac et al. reported competition of Al^{3+} ions with HREEs at pH~3.0 and low REE/HA ratios. At pH values around 5–6 and high REE/HA conditions, aluminum ions show a competitive behavior towards LREEs [35]. Similarly, Fe^{3+} preferentially binds to phenolic sites at pH 3, resulting in relatively lower adsorption of HREEs. At pH 6.0, Fe^{3+} competes with all REEs equally, decreasing the overall REE adsorption efficiency. Aside from the mentioned contaminants, other elements in the PLS likely impact the REE adsorption in a similar manner.

In order to fundamentally understand their adsorption behavior, the REEs were classified into light, middle, and heavy rare earth elements as shown in Figure 10. The data indicated that there was a convex pattern of improvement in RE content in the waste lignite after the adsorption experiment. As reported by Marsac et al., Al^{3+} and other contaminants preferentially bind to the phenolic and chelate ligands. This leaves carboxylic acids, such as acetic acids, to bind preferentially to MREEs, thereby resulting in the convex REE pattern [19]. Even though most of the Al and Fe content was removed during the aluminum precipitation stage, their total concentration was still approximately 20× higher than the REEs. As such, it is likely that primary consumption of binding sites by contaminants contributed towards a lower REE adsorption efficiency.

As per the Irving–Rossotti equations for REEs, the preferential binding of MREEs to the monocarboxylic ligands is a result of the large outer-sphere contribution in LREE- and MREE- complexation [19]. Based on the discussion presented previously, the higher HREE content increase relative to the LREE content was likely a result of the preferential consumption of carboxylic acid sites by aluminum [40]. Furthermore, Wang et al. reported that the bond length between humic acids and REEs decreases with an increase in atomic number from lanthanum to lutetium, whereas binding energy showed an upward trend. Consequently, it was concluded that the HREE and -OH bonds were more stable than LREE and -OH bonds [29].

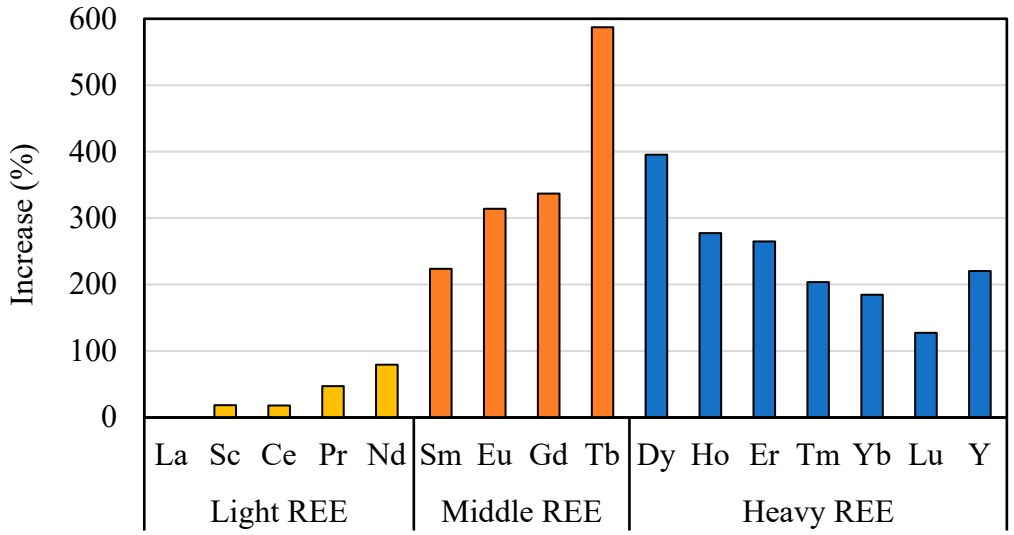

Figure 10. Increase in the light (LREE), middle (MREE), and heavy rare earth element (HREE) contents of the lignite waste material after the pilot plant adsorption test.

3.3. Process Flowsheet Development

The pilot-scale circuit demonstrated that the REEs adsorption stage provides promising means to generate a concentrated RE source. However, it was observed that the adsorption efficiency was approximately 30% which necessitated further processing of the solution to recover the remaining elements of interest in the solution. It was postulated that reduced adsorption efficiency was likely due to the amount of PLS treated per unit mass of lignite and limited residence time in the filter for the adsorption process. As such, another bench-scale experiment was conducted using the filtrate of the aluminum precipitation circuit at a 20% S/L ratio. The results demonstrated a significant improvement in the RE adsorption efficiency, thereby confirming the hypothesis that the adsorption efficiency was limited in the pilot scale test by the conditions (Figure 11). Based on these results, the preferred adsorption reactor is likely a well-mixed tank designed to provide adequate time for the adsorption process to run its course to near completion.

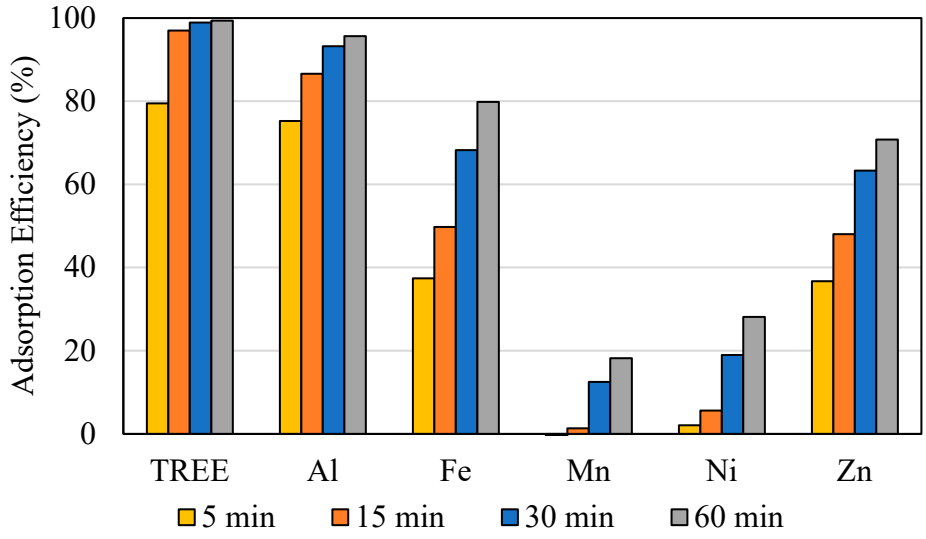

Figure 11. Adsorption efficiency of different elements of interest as a function of time using a 20% S/L ratio.

The adsorption kinetics were relatively fast with approximately 80% of the REEs adsorbed by the lignite within the first five minutes of the reaction. Increasing the time to

60 min improved the adsorption efficiency to 99%. The Al and Fe adsorption kinetics were equally fast, which corroborated the hypothesis that REEs compete with contaminant ions for the binding sites. Similarly, Mn, Ni, and especially Zn adsorption rates also increased. Simultaneously, the leaching recovery of calcium was 49% within the first five minutes of the reaction, signifying high calcium removal efficiency. However, as the reaction progressed, calcium started adsorbing on the solids and the leaching recovery decreased from 49% to −6% (signifying adsorption), indicating calcium loss from the PLS. Adsorption of calcium from the PLS by the adsorbent suggests an abundance of available binding sites even after adsorption of significant amounts of REE, Al, Fe and Zn contents. Similar to the previously presented bench-scale results, it was observed that the pH of the solution drifted to 5.0 within five minutes of the reaction. Based on the precipitation behavior of the contaminants (Figure 5), Al and Fe precipitation at pH 4.5 is expected to contribute to Al and Fe adsorption efficiency values. However, minimum REE precipitation occurs at the given pH value.

Based on the results, it can be concluded that the adsorption stage can be effectively used to recover REEs from the PLS solution. As such, a new flowsheet was developed, which includes further processing of the concentrated lignite material after the adsorption stage (Figure 12). The initial process circuit in the flowsheet is identical to the previous process flow presented in Figure 6. However, it should be noted that an additional iron precipitation stage at pH 3.2–3.4 prior to aluminum precipitation may be needed if the PLS contains elevated iron content to minimize the REE loss. Following the Al removal step, adsorption may be carried out with lignite on the remaining PLS using a reaction tank with pH control similar to the precipitation circuits. As indicated by the bench-scale data shown in Figure 11, elevated solids concentrations, i.e., 20%–30% S/L (w/v) and a retention time of around 15 min is recommended to ensure high adsorption efficiency. The new flowsheet does not process the filtrate after the adsorption stage as it will be essentially barren of REEs. However, if needed, it could be further processed to recover other critical metals in the solution following the process schematic shown in Figure 6.

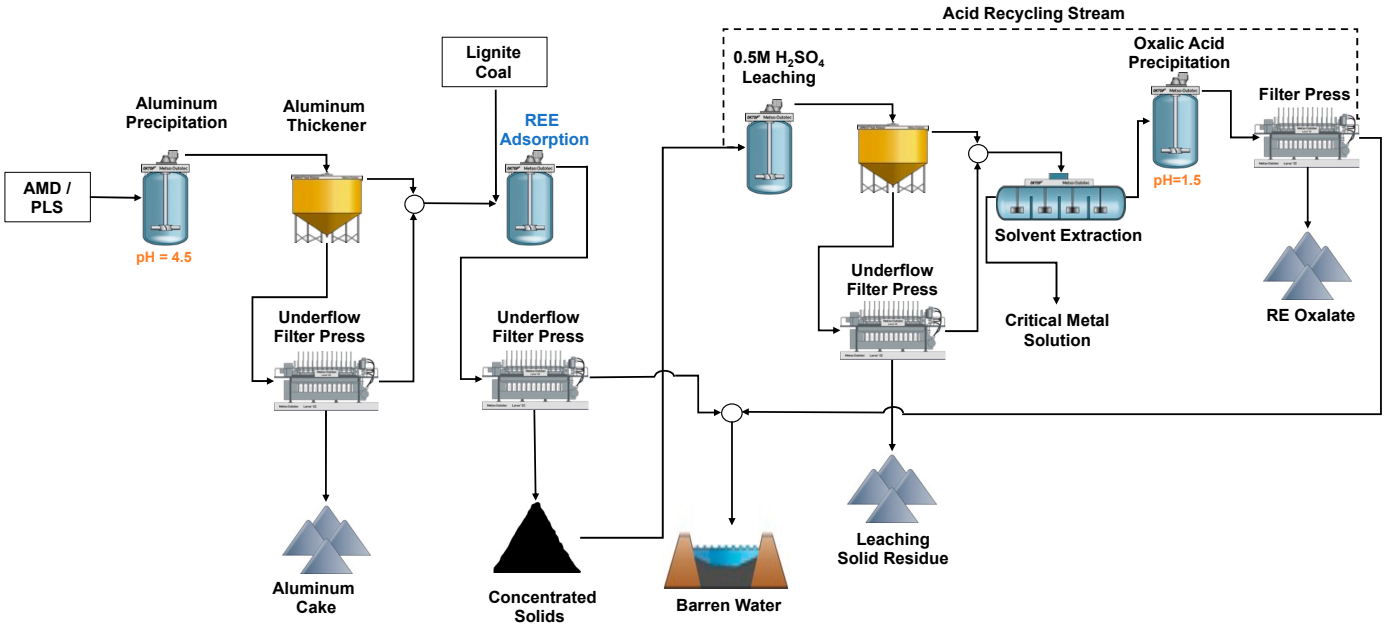

Figure 12. Proposed flowsheet for future studies to concentrate and subsequently extract and purify rare earth oxide.

The solids enriched in REE content will be leached using a 20%–30% S/L (w/v) ratio and dilute sulfuric acid (or other acids) of around 0.5 mol/L. Leaching of the concentrated solids obtained from the pilot scale test indicated that a PLS containing >200 ppm REE

concentration could be generated (Table 7). For comparison, bench scale testing of the untreated lignite material resulted in a PLS with only 66.6 ppm REE content at the same conditions, and leaching of bituminous coal sources typically produces a PLS containing less than 20 ppm [41]. Furthermore, the leachate contained elevated concentrations of other critical metals relative to the untreated solids leachate. The Co content remained unaffected due to the lack of adsorption in the pilot scale test. Hence, in contrast to the hundreds of gallons of relatively dilute PLS obtained from conventional leaching, processing of the enriched lignite will generate an upgraded PLS with significantly less volume, which should enhance economical viability for treating low-grade secondary sources from which the PLS is normally low in REE content.

Table 7. Comparison in the elemental concentrations (ppm) of PLS generated from the leaching of untreated and concentrated solids using 0.5 mol/L sulfuric acid at 20% S/L for 30 min.

	TREE	Co	Ni	Zn	Mn
Pre-Adsorption Leachate	66.6	56.2	159.3	43.0	106.9
Post-Adsorption Leachate	225.7	58.7	237.6	171.1	189.8

A detailed techno-economic analysis has been performed on the processing of PLS generated from coarse coal refuse using solvent extraction [41]. It was found that PLS processing cost (OPEX + CAPEX) could be reduced from 150 $/kg to 51 $/kg of mixed REE product with an increase in the PLS content from 65 ppm to 200 ppm using 0.5:1 organic-to-aqueous ratio (O:A). Based on the data presented, the processing of the enriched lignite will generate a PLS containing more than 200 ppm solution. Therefore, the processing cost for solvent extraction will decrease from 150 $/kg to less than 50 $/kg of high-purity REE product. However, since the bench scale results demonstrated the potential to achieve higher adsorption efficiencies, the PLS content is expected to be considerably higher than 200 ppm under optimized conditions, and therefore, further reductions in the processing cost are foreseen.

As for the contaminants in the leachate, primary contaminants are anticipated to be Ca, Al, and Fe. Even though calcium was adsorbed on the solids towards the end of the experiment, it is not anticipated to be a problem in solvent extraction due to the higher selectivity of extractants such as Cyanex 272 and D2EHPA towards REEs [42]. In contrast, ferric iron is one of the most problematic elements in solvent extraction when using Cyanex 272 [43]. However, if the iron is identified to be present in ferric form, steel wool or other reducing agents could be effectively used to reduce ferric iron to ferrous [44]. Alternatively, an extractant selective towards REEs in a ferric solution system could be employed. The stripped solution with primarily REEs could be processed using oxalic acid precipitation. The optimum operating pH in the oxalic acid precipitation stage was anticipated to be 1.5 to maximize REE product purity based on the previously published research [15,45]. The generated REE oxalates can be roasted at 750 °C for 2 h to generate high-purity rare earth oxides. The primary reason for oxalic acid use is its higher selectivity towards REEs. However, since the REE solution is anticipated to contain considerably lower contaminant content, alternative precipitants such as sodium carbonate could be used which will provide relatively better economics. The raffinate from the REE precipitation stage could be recycled completely or partially to re-leach the concentrated lignite coal.

As other critical metals such as Ni, Mn, and Zn were also adsorbed in the concentrated solids and their combined content was significantly higher than the REEs (Table 6), the REE barren PLS from SX can be further processed for their extraction. Li and Zhang showed that sodium sulfide shows high selectivity towards Co, Ni, and Zn and therefore can be effectively used to insolubilize these elements [46]. Subsequently, Mn can be recovered by increasing the solution pH to 9.0. Further separation and purification can be conducted using solvent extraction [46]. It should be noted that the PLS generated from the leaching of the enriched solids would be significantly smaller in volume than the AMD. As such,

the cost associated with the chemicals was expected to be substantially lower than the AMD treatment. Finally, since the humic acid is not solubilized in the acidic pH, there is a potential to reuse the solid residue for REE adsorption. However, further investigation is required to corroborate this claim.

4. Conclusions

A waste lignite source produced during the production of construction sand was found to be concentrated in rare earth elements (REEs) and other critical elements such as cobalt, nickel, and zinc. When submersing the lignite material in a dilute solution of REEs and contaminant elements, the REE content in the material was increased by over 100% with heavy REE enrichment being by nearly 250%, which was attributed to the chelating properties of humic acid in the lignite with the REEs. The dilute solution was the pregnant leachate generated from the leaching of Baker seam coarse refuse. Furthermore, a preliminary leaching study conducted using 1% S/L (%w/v) at 75 °C for 2 h at various lixiviant concentrations revealed that REEs in the lignite material were easily leached using mild acid conditions. For instance, REE recovery improved from 32% to nearly 90% when the sulfuric acid concentration increased from 0.01 mol/L to 0.1 mol/L.

Based on these findings, a pilot-scale test program was performed using the lignite waste to adsorb the REEs and other critical elements from a pregnant leach solution produced from a test heap leach pad that was comprised of 2000 tons of coarse coal refuse. The PLS was initially treated by pH control to remove the iron and aluminum by precipitation. The filtrate produced from the filtration of aluminum precipitate was passed through a high-pressure plate-and-frame filter filled with lignite waste. The adsorption efficiency was approximately 30 percent for REEs and all the remaining REEs were recovered in a RE-CM precipitation circuit using a solution pH value of 9.0. The low adsorption efficiency was primarily due to the large volume of PLS treated per unit of lignite mass as well as the limited residence time. Subsequent to the pilot plant test, a benchtop test was performed which revealed that nearly 96% of the REEs in the heap leach PLS can be adsorbed by the lignite material within 15 min in a stirred reactor mixing a 20% solid by weight slurry having a pH of 4.5. Contaminants such as Fe and Al were found to compete for the binding sites associated with the humic acid in the lignite material and thus reduce REE adsorption efficiency. Calcium, which was a primary contaminant in the lignite, was effectively removed during the adsorption stage.

Based on the results, a new process flowsheet was proposed which utilizes the lignite waste as a means to elevate the REE concentration in the PLS that is fed to downstream separation and purification processes. As a result, reductions in CAPEX and OPEX are anticipated, thereby enhancing the economic viability of rare earth element recovery from a low-grade secondary source. Furthermore, leaching of the lignite material at high percent solids will generate an REE-concentrated PLS that can be processed using solvent extraction and/or oxalic acid precipitation to generate high-purity rare earth oxide in a more efficient manner. Finally, the solution remaining after the adsorption stage can be further processed to generate high-purity products of Co, Ni, Zn, and Mn.

Supplementary Materials: The following supporting information can be downloaded at: https://www.mdpi.com/article/10.3390/min13070921/s1, Figure S1: Leaching characteristics of individual rare earth elements as a function of varying sulfuric acid concentrations (mol/L); Table S1: Individual REE content in the lignite material screened at 30 mesh.

Author Contributions: A.N.: Conceptualization, Formal analysis, Investigation, Writing—original draft, Writing—review and editing, Project administration. R.H.: Conceptualization, Methodology, Writing—review and editing, Supervision, Project administration, Funding acquisition. All authors have read and agreed to the published version of the manuscript.

Funding: This material is based upon work supported by the Department of Energy Award Number DE-FE0031827.

Data Availability Statement: The data presented in this study is available on request from the corresponding author.

Conflicts of Interest: The authors declare no conflict of interest.

References

1. Van Gosen, B.S.; Verplanck, P.L.; Seal, R.R., II; Long, K.R.; Gambogi, J. *Rare-Earth Elements*; US Geological Survey: Reston, VA, USA, 2017.
2. Jha, M.K.; Kumari, A.; Panda, R.; Kumar, J.R.; Yoo, K.; Lee, J.Y. Review on Hydrometallurgical Recovery of Rare Earth Metals. *Hydrometallurgy* **2016**, *165*, 2–26.
3. Zhang, W.; Noble, A.; Yang, X.; Honaker, R. A Comprehensive Review of Rare Earth Elements Recovery from Coal-Related Materials. *Minerals* **2020**, *10*, 451.
4. Peiravi, M.; Ackah, L.; Guru, R.; Mohanty, M.; Liu, J.; Xu, B.; Zhu, X.; Chen, L. Chemical Extraction of Rare Earth Elements from Coal Ash. *Miner. Metall. Process.* **2017**, *34*, 170–177.
5. Montross, S.N.; Yang, J.; Britton, J.; McKoy, M.; Verba, C. Leaching of Rare Earth Elements from Central Appalachian Coal Seam Underclays. *Minerals* **2020**, *10*, 577.
6. Pan, J.; Nie, T.; Zhou, C.; Yang, F.; Jia, R.; Zhang, L.; Liu, H. The Effect of Calcination on the Occurrence and Leaching of Rare Earth Elements in Coal Refuse. *J. Env. Chem. Eng.* **2022**, *10*, 108355.
7. Eterigho-Ikelegbe, O.; Harrar, H.; Bada, S. Rare Earth Elements from Coal and Coal Discard—A Review. *Min. Eng.* **2021**, *173*, 107187.
8. Banerjee, R.; Chakladar, S.; Mohanty, A.; Chattopadhyay, S.K.; Chakravarty, S. Leaching Characteristics of Rare Earth Elements from Coal Ash Using Organosulphonic Acids. *Min. Eng.* **2022**, *185*, 107664.
9. Pan, J.; Hassas, B.V.; Rezaee, M.; Zhou, C.; Pisupati, S.V. Recovery of Rare Earth Elements from Coal Fly Ash through Sequential Chemical Roasting, Water Leaching, and Acid Leaching Processes. *J. Clean. Prod.* **2021**, *284*, 124725.
10. Zhang, W.; Honaker, R. Calcination Pretreatment Effects on Acid Leaching Characteristics of Rare Earth Elements from Middlings and Coarse Refuse Material Associated with a Bituminous Coal Source. *Fuel* **2019**, *249*, 130–145.
11. Zhang, W.; Honaker, R. Characterization and Recovery of Rare Earth Elements and Other Critical Metals (Co, Cr, Li, Mn, Sr, and V) from the Calcination Products of a Coal Refuse Sample. *Fuel* **2020**, *267*, 117236.
12. Gupta, T.; Nawab, A.; Honaker, R. Pretreatment of Bituminous Coal By-Products for the Hydrometallurgical Extraction of Rare Earth Elements. *Minerals* **2023**, *13*, 614.
13. Gupta, T.; Nawab, A.; Honaker, R. Removal of Iron from Pyrite-Rich Coal Refuse by Calcination and Magnetic Separation for Hydrometallurgical Extraction of Rare Earth Elements. *Minerals* **2023**, *13*, 327. [CrossRef]
14. Ji, B.; Li, Q.; Zhang, W. Rare Earth Elements (REEs) Recovery from Coal Waste of the Western Kentucky No. 13 and Fire Clay Seams. Part I: Mineralogical Characterization Using SEM-EDS and TEM-EDS. *Fuel* **2022**, *307*, 121854. [CrossRef]
15. Nawab, A.; Yang, X.; Honaker, R. An Acid Baking Approach to Enhance Heavy Rare Earth Recovery from Bituminous Coal-Based Sources. *Min. Eng.* **2022**, *184*, 107610. [CrossRef]
16. Haysahi, K.; Shibata, H.; Yui, M.; Ohmoto, H. Experimental Study Assessing the Role of Sedimentary Organic Materials to Control the Redox State of Ground Materials to Control the Redox State of Groundwater: Consumption of Dissolved Oxygen by Humic Acid. *Resour. Geol.* **2001**, *51*, 45–54.
17. Szymański, K.; Morawski, A.W.; Mozia, S. Humic Acids Removal in a Photocatalytic Membrane Reactor with a Ceramic UF Membrane. *Chem. Eng. J.* **2016**, *305*, 19–27. [CrossRef]
18. Laudal, D.A.; Benson, S.A.; Addleman, R.S.; Palo, D. Leaching Behavior of Rare Earth Elements in Fort Union Lignite Coals of North America. *Int. J. Coal Geol.* **2018**, *191*, 112–124.
19. Marsac, R.; Catrouillet, C.; Davranche, M.; Bouhnik-Le Coz, M.; Briant, N.; Janot, N.; Otero-Fariña, A.; Groenenberg, J.E.; Pédrot, M.; Dia, A. Modeling Rare Earth Elements Binding to Humic Acids with Model VII. *Chem. Geol.* **2021**, *567*, 120099. [CrossRef]
20. Wan, Y.; Liu, C. The Effect of Humic Acid on the Adsorption of REEs on Kaolin. *Colloids Surf. A Physicochem. Eng. Asp.* **2006**, *290*, 112–117. [CrossRef]
21. Wang, X.; Deng, F.; Cheng, H.; Ning, S.; Li, B.; Pan, S.; Yin, X. Effects of Heating on the Binding of Rare Earth Elements to Humic Acids. *Energies* **2022**, *15*, 7362. [CrossRef]

22. Erdogan, S.; Baysal, A.; Akba, O.; Hamamci, C. Interaction of Metals with Humic Acid Isolated from Oxidized Coal. *Pol. J. Env. Stud.* **2007**, *16*, 617–675.
23. Marzouk, N.M.; Soliman, M.S.; El-tanahy, A.M.M.; Mounir, A.M. Effect of Both Potassium Phosphate and Zinc Nanocomposites Prepared via Gamma Radiation on Growth and Productivity of Potato under New Reclaimed Soils. *Egypt. J. Chem.* **2022**, *65*, 1–2.
24. Hamad, H.A.; AbdElhafez, S.E.; Elsenety, M.M.; Sorour, M.K.; Amin, N.K.; Abdelwahab, O.; El-Ashtoukhy, E.-S.Z. Fabrication and Characterization of Functionalized Lignin-Based Adsorbent Prepared from Black Liquor in the Paper Industry for Superior Removal of Toxic Dye. *Fuel* **2022**, *323*, 124288. [CrossRef]
25. Rosenthal, M. *A Unique Collaboration of Coal-Based REEs and the U.S.'s Largest Rare Earth Producer*; Final Technical Report, Project Number: 89243320CFE000053-0001; MP Materials/Department of Energy: Las Vegas, NV, USA, 2022; 221p.
26. Gupta, T. Oxidation Pretreatment for Enhanced Leachability of Rare Earth Elements from Bituminous Coal Sources. Ph.D. Thesis, University of Kentucky, Lexington, KY, USA, 2021.
27. Yang, X. Leaching Characteristics of Rare Earth Elements from Bituminous Coal-Based Sources. Ph.D. Thesis, University of Kentucky, Lexington, KY, USA, 2019. [CrossRef]
28. Shi, Q.; Zhao, Y.; Meng, X.; Shen, L.; Qiu, G.; Zhang, X.; Yu, H.; He, X.; He, H.; Zhao, H. Column Leaching of Ion Adsorption Rare Earth Ore at Low Ammonium Concentration. *J. Mater. Res. Technol.* **2022**, *19*, 2135–2145. [CrossRef]
29. Wang, X.; Cheng, W.; Xu, R. Adsorption of Rare Earth Elements on Organic Matter in Coal. *J. Rare Earths* **2022**, *41*, 1108–1115. [CrossRef]
30. Xiao, L.; Li, Y.; Liao, Y.; Ma, H.; Wu, J.; Zhang, Y.; Yao, J. Bioconversion of Lignite Humic Acid by White-Rot Fungi and Characterization of Products. *3 Biotech* **2018**, *8*, 258.
31. Pourret, O.; Davranche, M.; Gruau, G.; Dia, A. Competition between Humic Acid and Carbonates for Rare Earth Elements Complexation. *J. Colloid. Interface Sci.* **2007**, *305*, 25–31.
32. Dia, A.; Gruau, G.; Olivié-Lauquet, G.; Riou, C.; Molénat, J.; Curmi, P. The Distribution of Rare Earth Elements in Groundwaters: Assessing the Role of Source-Rock Composition, Redox Changes and Colloidal Particles. *Geochim. Cosmochim. Acta* **2000**, *64*, 4131–4151.
33. Tang, J.; Johannesson, K.H. Speciation of Rare Earth Elements in Natural Terrestrial Waters: Assessing the Role of Dissolved Organic Matter from the Modeling Approach. *Geochim. Cosmochim. Acta* **2003**, *67*, 2321–2339.
34. Marsac, R.; Davranche, M.; Gruau, G.; Dia, A.; Pédrot, M.; Le Coz-Bouhnik, M.; Briant, N. Effects of Fe Competition on REE Binding to Humic Acid: Origin of REE Pattern Variability in Organic Waters. *Chem. Geol.* **2013**, *342*, 119–127.
35. Marsac, R.; Davranche, M.; Gruau, G.; Dia, A.; Bouhnik-Le Coz, M. Aluminium Competitive Effect on Rare Earth Elements Binding to Humic Acid. *Geochim. Cosmochim. Acta* **2012**, *89*, 1–9.
36. Li, Q.; Ji, B.; Honaker, R.; Noble, A.; Zhang, W. Partitioning Behavior and Mechanisms of Rare Earth Elements during Precipitation in Acid Mine Drainage. *Colloids Surf. A Physicochem. Eng. Asp.* **2022**, *641*, 128563. [CrossRef]
37. Sonke, J.E.; Salters, V.J.M. Lanthanide–Humic Substances Complexation. I. Experimental Evidence for a Lanthanide Contraction Effect. *Geochim. Cosmochim. Acta* **2006**, *70*, 1495–1506.
38. Marsac, R.; Davranche, M.; Gruau, G.; Dia, A. Metal Loading Effect on Rare Earth Element Binding to Humic Acid: Experimental and Modelling Evidence. *Geochim. Cosmochim. Acta* **2010**, *74*, 1749–1761.
39. Nawab, A.; Yang, X.; Honaker, R. Parametric Study and Speciation Analysis of Rare Earth Precipitation Using Oxalic Acid in a Chloride Solution System. *Min. Eng.* **2022**, *176*, 107352. [CrossRef]
40. Marsac, R.; Davranche, M.; Gruau, G.; Bouhnik-Le Coz, M.; Dia, A. An Improved Description of the Interactions between Rare Earth Elements and Humic Acids by Modeling: PHREEQC-Model VI Coupling. *Geochim. Cosmochim. Acta* **2011**, *75*, 5625–5637. [CrossRef]
41. Honaker, R.; Werner, J.; Nawab, A.; Zhang, W.; Noble, A.; Free, M.; Yang, X. *Demonstration of Scaled-Production of Rare Earth Oxides and Critical Materials from Coal-Based Sources*; US Department of Energy: Washington, DC, USA, 2023.
42. Innocenzi, V.; De Michelis, I.; Ferella, F.; Vegliò, F. Secondary Yttrium from Spent Fluorescent Lamps: Recovery by Leaching and Solvent Extraction. *Int. J. Min. Process* **2017**, *168*, 87–94. [CrossRef]
43. Zhang, K.; Qiu, L.; Tao, J.; Zhong, X.; Lin, Z.; Wang, R.; Liu, Z. Recovery of Gallium from Leach Solutions of Zinc Refinery Residues by Stepwise Solvent Extraction with N235 and Cyanex 272. *Hydrometallurgy* **2021**, *205*, 105722. [CrossRef]
44. Santos-Juanes, L.; García-Ballesteros, S.; Vercher, R.F.; Amat, A.M.; Arques, A. Commercial Steel Wool Used for Zero Valent Iron and as a Source of Dissolved Iron in a Combined Red-Ox Process for Pentachlorophenol Degradation in Tap Water. *Catal. Today* **2019**, *328*, 252–258. [CrossRef]
45. Chi, R.; Xu, Z. Solution Chemistry Approach to the Study of Rare Earth Element Precipitation by Oxalic Acid. *Metall. Mater. Trans. B* **1999**, *30*, 189–195. [CrossRef]
46. Li, Q.; Zhang, W. Process Development for Recovering Critical Elements from Acid Mine Drainage. *Resour. Conserv. Recycl.* **2022**, *180*, 106214. [CrossRef]